PCCP

ROYAL SOCIETY OF CHEMISTRY

PAPER

View Article Online
View Journal | View Issue

Cite this: *Phys. Chem. Chem. Phys.*, 2024, **26**, 12573

Beryllium carbonyl $Be(CO)_n$ (n = 1–4) complex: a p-orbital analogy of Dewar–Chatt–Duncanson model†

Siddhartha K. Purkayastha, [a] Shahnaz S. Rohman,[b] Pattiyil Parameswaran *[b] and Ankur K. Guha *[a]

Received 1st March 2024,
Accepted 19th March 2024

DOI: 10.1039/d4cp00908h

rsc.li/pccp

Transition metal–carbonyl bonds are rationalized by M ← CO σ donation and M → CO π back donation where the d orbital of the transition metal is involved. This bonding model provided by Dewar, Chatt and Duncanson (DCD) has rationalized many transition metal–ligand bonds. The involvement of p orbital in such a DCD model can be intriguing. Alkaline earth metals with ns^2np^0 configuration may appear suitable as ns^0np^2 excitation has been recognized in many complexes. Herein, a theoretical study is presented for the $Be(CO)_n$ (n = 1–4) complex to verify this assumption. Detailed electronic structure analyses confirmed the involvement of the p orbital of beryllium in M → CO π back donation, thereby supporting the hypothesis. EDA-NOCV results reveal that the π-back donation from the central Be atom to CO ligands significantly predominates over the σ donation from the ligands for both $Be(CO)_3$ and $Be(CO)_4$. Our calculations reveal that $Be(CO)_4$ is the highest carbonyl that may be experimentally detected.

Introduction

Bonding in metal carbonyls is generally rationalized by the Dewar–Chatt–Duncanson model,[1,2] where M ← CO σ donation and M → CO π back donation take place simultaneously. This synergistic bonding situation (Scheme 1a) results in the weakening of the CO bond, which can be traced using IR spectroscopy. This bonding situation was first introduced by Dewar[1] in 1951 to explain the peculiar structure of Zeise's salt $PtCl_3(C_2H_4)^-$. The Dewar–Chatt–Duncanson (DCD) model has become the standard bonding model of transition metal complexes.[3]

Generally, transition metal having d orbital is best suited for this type of bonding, which favours backdonation from the filled d orbital to π* orbital of the CO ligand. However, an alternative situation may also be envisioned where the metal uses its filled p_z-orbital for the M → CO (π*) back donation (Scheme 1b) and vacant s, p_x and p_y orbitals of metal for M ← CO σ donation. To realize this, the choice of the metal is very crucial. One such obvious choice is alkaline earth metal, among which beryllium is very lucrative. Braunschweig and co-workers have reported the first example of neutral zero valent beryllium complex L–Be–L (L = cyclic (alkyl)(amino)carbene).[4] The bonding situation was described as a donor–acceptor interaction between the ground state of L ligands and Be(0), which is in $1s^22s^02p^2$ electronic configuration.[4] Similarly, the $OCBe(CO)_3$ complex has also been reported by Chen *et al.*[5] This indicates that beryllium can show a bonding feature involving its excited $1s^22s^02p^2$ electronic configuration where the valence 2s orbital is empty and 2p orbital is filled, a perfect match to fulfill the hypothetical bonding situation in Scheme 1b. It should be noted that Be(0) compounds have been predicted theoretically.[6,7] However, to the best of our knowledge, such a connection between the p-orbital analogy of the DCD model has never been highlighted in those Be(0) compounds; however, in this study, the beryllium carbonyl complex, $Be(CO)_n$ (n = 1–4), has been theoretically studied, and it shows such a bonding situation. Involvement of beryllium 2s, $2p_x$ and $2p_y$ orbitals in M ← CO σ donation and $2p_z$ orbital in M → CO (π*) back donation is clearly established.

[a] *Advanced Computational Chemistry Centre, Cotton University, Panbazar, Guwahati, Assam, 781001, India. E-mail: ankurkantiguha@gmail.com*
[b] *Department of Chemistry, National Institute of Technology Calicut, Kozhikode, 673601, India. E-mail: param@nitc.ac.in*

† Electronic supplementary information (ESI) available: Fig. S1 and S2 and cartesian coordinates of all the optimized geometries. See DOI: https://doi.org/10.1039/d4cp00908h

Computational details

Geometry optimization and vibrational frequency calculations were performed using TPSSh/def2-TZVP[8] and M06-2X/def2-TZVP[9] levels in both singlet and triplet spin states. Zero-point

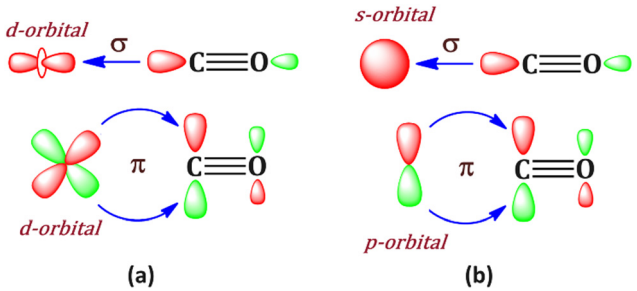

Scheme 1 Bonding situation in (a) transition metal carbonyls where d orbitals are involved and (b) bonding situation in metal carbonyls where s and p orbital of metal are involved.

corrections were included in bond dissociation energy calculations. All these calculations were performed using the Gaussian 16 suite program.[10] Single point CCSD(T)/cc-pVTZ calculations on TPSSh/def2-TZVP optimized geometries were performed using the ORCA 4.2.1 program.[11,12] We checked the multireference character using the T_1 diagnostic value of the converged CCSD wavefunction. They are smaller than the prescribed threshold (0.02), indicating a single reference character of the studied systems. Electron localization function (ELF)[13,14] calculation was performed using the Multiwfn program code.[15]

Energy decomposition analysis[16] in conjunction with the natural orbital for chemical valence[17] (EDA-NOCV) was performed at the BP86/TZ2P level[18] using the ADF2020.102 program package[19] on TPSSh optimized geometries. The interaction energy between fragments A and B in the molecule A–B can be considered as an indicator of bond strength between the two fragments under consideration. EDA mainly focuses on the intrinsic interaction energy (ΔE_{int}). This interaction energy is related to another physical observable, the bond dissociation energy (D_e), as can be seen in the following equation:

$$\Delta E_{int} = -D_e + \Delta E_{prep}$$

where $\Delta E_{prep} = (E_A^{GS} + E_B^{GS}) - (E_A + E_B)$

The fragments A and B in their respective ground states are excited to the frozen electronic and geometric states in the molecule A–B by providing them the required excitation energy (ΔE_{prep}). E_A^{GS} and E_B^{GS} refer to the electronic energy of the fragments A and B in their respective ground states, while E_A and E_B refer to the electronic energy of the corresponding fragments in their frozen geometries of the molecule.

The instantaneous interaction energy (ΔE_{int}) of a bond A–B is partitioned into chemically meaningful components as follows:

$$\Delta E_{int} = \Delta E_{elect} + \Delta E_{Pauli} + \Delta E_{orb} + \Delta E_{disp}.$$

The term ΔE_{elect} refers to the quasi-classical electrostatic interactions. The frozen electron density distribution of the fragments in the geometry of the molecules is calculated by quantum mechanics, and the interaction between the nuclei and electrons is calculated by classical laws. It is usually an attractive component and gives an estimate of electrostatic interactions that are excluded from the orbital-based analysis. ΔE_{Pauli} corresponds to the repulsive interactions between fragments of like spin as they approach each other. However, note that this term is not indicative of ionic bonding and is calculated by the anti-symmetrization and renormalization of the Kohn–Sham determinant of the orbitals. ΔE_{orb} is associated with the stabilization of orbitals during bond formation and is an attractive component. It includes the effects of charge transfer, relaxation, and polarization by deformation of the charge distribution of the fragments during bond formation.

Developed by Mitoraj and Michalak, the EDA-NOCV scheme further decomposes ΔE_{orb} term into contributions from each

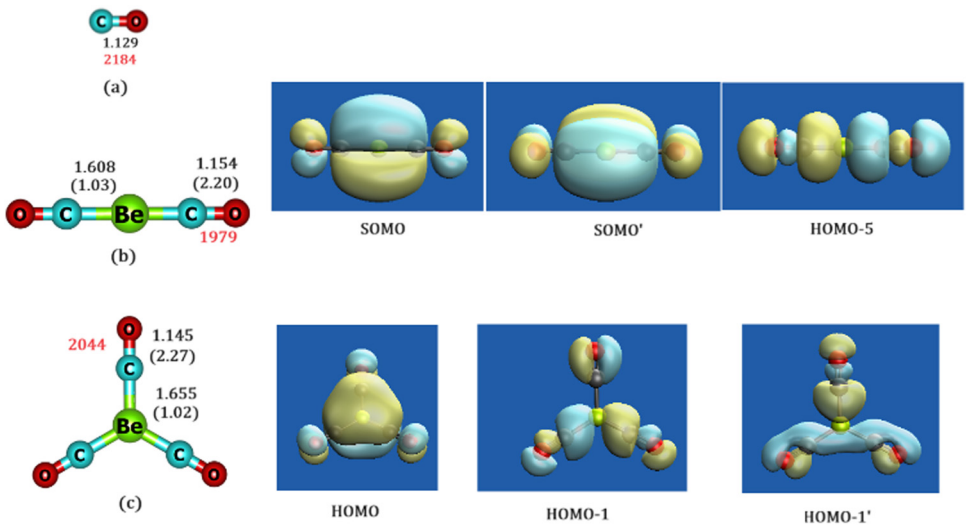

Fig. 1 Optimized geometries of (a) free CO (b) triplet $Be(CO)_2$ and (c) singlet $Be(CO)_3$ complex. Bond lengths are in Å, Mayer's bond orders are in parenthesis and IR active CO stretching frequencies (cm^{-1}) in red font. Shapes of the molecular orbitals responsible for Be ($2p_z$) → CO (π*) back donation and M ← CO σ donation are also shown.

irreducible representation in the point group of the interacting system. The natural orbitals for chemical valence (NOCV) provide insight into each specific orbital interaction between the fragments and the contribution of each pair of the interacting orbitals (Ψ_{-n}/Ψ_n) to the total bond energy. Within this scheme, ΔE_{orb} is expressed in terms of NOCVs as

$$\Delta E_{\mathrm{orb}} = \sum_{n=1}^{N/2} \Delta E_{\mathrm{orb}} = \sum_{n=1}^{N/2} v_n \left[-F^{\mathrm{TS}}_{-n,-n} + F^{\mathrm{TS}}_{n,n} \right]$$

where $-F^{\mathrm{TS}}_{-n,-n}$ and $F^{\mathrm{TS}}_{n,n}$ are the Kohn–Sham matrix elements defined over NOCV pairs with eigenvalues $-v_n$ and v_n, respectively, with respect to the transition-state density. This transition-state density is the intermediate density between that of the molecule and the superimposed fragments. The orbitals with a negative value exhibit antibonding nature and those with a positive value exhibit bonding nature. The strength of the pairwise orbital interactions can be quantitatively estimated and the associated change in charge density can be visualized *via* deformation densities.

Results and discussion

Let us start with the BeCO molecule (Fig. 1). Both TPSSh and M06-2X show similar geometrical features; hence, the discussion throughout the text will be based on TPSSh results. Although the optimized geometry of BeCO shows a strongly bonded complex in a triplet ground state, it is unstable with respect to separated Be and CO. This is in tune with previous experimental observations.[20] Moreover, the triplet ground state of BeCO provides a hint that the excitation from the $2s^2$ configuration of beryllium to $2s^12p^1$ takes place in the presence of a single CO ligand. Therefore, it is expected that the addition of another CO ligand will create more excitation of beryllium electron configuration and may reach the desired $2s^02p^2$ configuration. Indeed, the linear triplet $Be(CO)_2$ complex is stable with respect to dissociation to Be (^{1}S) and two CO molecules (bond dissociation energy is 40.2 kcal mol^{-1} for the loss of two CO molecules). Previous theoretical calculations by Sunil *et al.* confirmed this fact, further predicting that a stable dimer of $Be(CO)_2$ having a Be=Be double bonded complex may be realized in D_{2h} $(CO)_2BeBe(CO)_2$ species in the ^1A_g, ground state.[21] However, there is a difference in the geometry of the $Be(CO)_2$ complex. The present study predicts it to have a linear $D_{\infty h}$ geometry while the calculation of Sunil *et al.* at the HF level predicted a C_{2v} geometry.[21] In fact, no local minimum in the C_{2v} geometry of $Be(CO)_2$ is found at the TPSSh/def2-TZVP level. This might be due to the non-inclusion of the electron correlation in predicting the geometry.[21] To confirm this, we have optimized the geometry of $Be(CO)_2$ at CCSD(T)/cc-pVTZ, which could not locate any C_{2v} geometry, rather it locates a linear $D_{\infty h}$ geometry. We therefore prefer to discuss the linear $D_{\infty h}$ geometry of $Be(CO)_2$. The Be–C bond length in $Be(CO)_2$ is 1.608 Å and the CO bond is extremely elongated, resulting in a dramatic lowering of the IR active CO stretching frequency in the complex. This indicates a significant Be (2p) → CO (π*) back donation. The next addition of another CO to triplet $Be(CO)_2$ results in trigonal planar $Be(CO)_3$ complex. Remarkably, the singlet state is 18.6 kcal mol^{-1} more stable than the triplet. Both the structure and stability of $Be(CO)_3$ have been previously explored using BP86/def2-TZVPP and M06-2X/def2-TZVPP levels.[7] Significant reduction in CO stretching frequency is observed and the molecular orbital analysis confirmed the Be(2p) → CO (π*) back donation. It should be noted that both $Be(CO)_2$ and $Be(CO)_3$ were experimentally identified.[20]

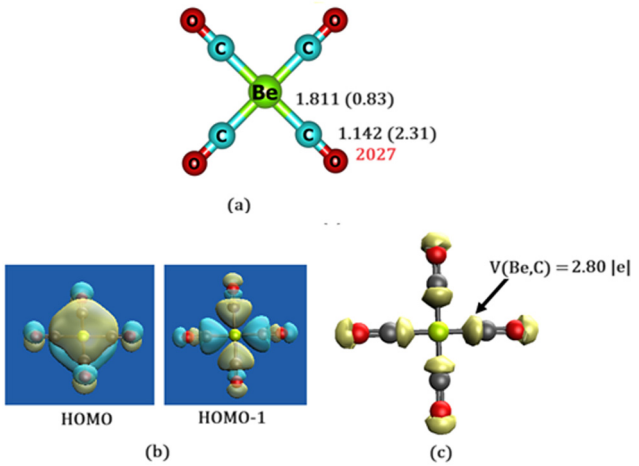

Fig. 2 (a) Optimized geometry of $Be(CO)_4$ complex. Bond lengths are in Å, Mayer's bond orders are in parenthesis and IR active CO stretching frequencies (cm^{-1}) in red font, (b) shapes of HOMO and HOMO−1 and (c) ELF disynaptic V(Be,C) basin with population in |e| of the $Be(CO)_4$ complex.

Let us turn our attention now to $Be(CO)_4$. It adopts a perfectly square planar geometry in its singlet electronic ground state (Fig. 2a). The triplet state is 10.7 kcal mol^{-1} higher in energy at TPSSh/def2-TZVP and 14.2 kcal mol^{-1} at the CCSD(T)/cc-pVTZ//TPSSh/def2-TZVP level. The tetrahedral geometry is also a saddle point on the potential energy surface. All other manually constructed isomers are also saddle points on the potential energy surface. It implies that the square planar geometry of $Be(CO)_4$ is the lowest energy structure. While BeCO has a triplet ground state,[20] the ground state of $Be(CO)_4$ is a closed-shell singlet. Moreover, while the triplet electronic states of BeCO and $Be(CO)_2$ are more stable, singlet electronic states become more stable for $Be(CO)_3$ and $Be(CO)_4$ complexes. All Be–C bond lengths in $Be(CO)_4$ are equal (1.811 Å) at the TPSSh level. Moreover, M06-2X level produces similar Be–C distances (1.816 Å). Mayer's bond order for the Be–C bond is 0.83, indicating significant covalency and a stronger Be–CO bond. The computed Hirshfeld charge at the Be atom is near zero (−0.05 *e*) and slightly positive (0.1 *e*) at the carbon atom indicating that the bonding situation should not be described as $Be^+(CO)_4^-$ or $Be^{2+}(CO)_4^{2-}$, rather as common DCD model, which recovers covalency in the metal–ligand bond.[1,2] The CO bond is elongated by 0.013 Å compared to its length in the free form (1.129 Å). This reflects Be → CO back donation, which is also evident from the lowering of the IR active stretching frequency (unscaled) of the CO group (2027 cm^{-1}) compared to its free value (2184 cm^{-1}). The calculated bond dissociation

Table 1 EDA-NOCV results (in kcal mol^{-1}) of $Be(CO)_3$ and $Be(CO)_4$ at the BP86/TZ2P level of theory

		$Be(CO)_3$		$Be(CO)_4$
Fragment 1		$Be(1s^2 2s^0 2p_z^2)$		$Be(1s^2 2s^0 2p_z^2)$
Fragment 2		3CO		4CO
ΔE_{int}		−256.3		−266.8
ΔE_{Pauli}		69.2		37.9
ΔE_{elstat} [a]		−87.0 (26.9%)		−78.7 (26%)
ΔE_{disp}		−1.8		−1.9
ΔE_{orb} [a]		−236.7 (73.1%)		−224.1 (74%)
ΔE_σ [b]	$\Delta E_{\sigma(+\,+\,+)}$ [b]	−17.1 (7.2%)	$\Delta E_{\sigma(+\,+\,+)}$ [b]	−18.2 (8.1%)
	$\Delta E_{\sigma(+\,-\,+)}$ [b]	−40.3 (17.0%)	$\Delta E_{\sigma(\cdot\,+\,-)}$ [b]	−32.8 (14.6%)
	$\Delta E_{\sigma(+\,\cdot\,-)}$ [b]	−40.3 (17.0%)	$\Delta E_{\sigma(+\,-\,\cdot)}$ [b]	−32.8 (14.6%)
			$\Delta E_{\sigma(+\,-\,+\,-)}$ [b]	−8.1 (3.6%)
ΔE_π [b]		−128.3 (54.2%)		−123.7 (55.3%)
ΔE_{rest} [c]		−10.7 (4.6%)		−8.5 (3.8%)
ΔE_{prep}		179.2		196.6
$-D_e$ [d]		−77.1		−70.2

[a] The values in parentheses give the percentage contribution to the total attractive interactions $\Delta E_{elstat} + \Delta E_{orb}$. [b] The values in parentheses give the percentage contribution to the total orbital interactions ΔE_{orb}. [c] $\Delta E_{rest} = \Delta E_{orb} - (\Delta E_\sigma + \Delta E_\pi)$. [d] Dissociation energy (D_e).

energy for the loss of four molecules of CO from $Be(CO)_4$ is 65.6 kcal mol^{-1} (46.2 kcal mol^{-1} at CCSD(T)/cc-pVTZ level), indicating that the Be–CO bonds are stronger. This indicates that the possibility of its experimental observation may be in the low-temperature neon matrix where the isolation of $M(CO)_8$ (M = Ca, Sr or Ba) has been reported.[22]

Fig. 2b shows the shapes of the highest occupied molecular orbital (HOMO) and HOMO−1 of $Be(CO)_4$ complex. HOMO represents the Be → CO π* back donation and is delocalized among all four carbon centres. This delocalization stabilizes the square planar geometry over the tetrahedral one. HOMO−1 represents the CO → Be σ donation, thereby establishing the synergism observed in the common DCD model. Interestingly, the Be → CO π* back donation involves Be $2p_z$ orbital. Thus, the present bonding situation can be considered as a p-orbital analog of the DCD model. Electron localization function (ELF)[12,13] analysis also reveals the presence of disynaptic V(Be,C) basins with a population greater than 2.00 |e| (Fig. 2c), indicating a partial double Be–C bonding character. The bonding situation is exactly similar to that observed for the experimentally observed neutral zero valent beryllium complex L–Be–L (L = cyclic (alkyl)(amino)carbene)[4] and $OCBe(CO)_3$ complex[5] and theoretically proposed Be(0) compounds.[6,7]

Are higher carbonyl complexes possible? We tried to optimize $Be(CO)_n$ with n = 5–8 in both singlet and triplet electronic states. However, geometry optimisation leads to dissociation of CO ligand(s). This indicates that the beryllium atom can accommodate a maximum of four CO groups.

To gain an insight into the quantitative nature of the bonding description in $Be(CO)_3$ and $Be(CO)_4$, we carried out energy decomposition analysis coupled with natural orbital for chemical valence (EDA-NOCV). In both the systems, the central beryllium atom in $1s^2 2s^0 2p_z^2$ electronic state is considered as one fragment and the ground state singlet carbonyl ligands, namely, three CO ligands in $Be(CO)_3$ and four CO ligands in $Be(CO)_4$, as another fragment. The bonding scheme considered here features purely dative interactions, with σ-donations from the CO ligands and π-back donations from the central beryllium atom (Table 1).

The interaction energy ΔE_{int}, which can be considered as a measure of the Be–C bond strength, is found to be only slightly higher for $Be(CO)_4$ (−266.8 kcal mol^{-1}) as compared to $Be(CO)_3$ (−256.3 kcal mol^{-1}). Note that the total attractive component of interaction energy is higher for $Be(CO)_3$. The slightly higher value of ΔE_{int} for $Be(CO)_4$ mainly arises from the significantly lower value of Pauli repulsion (37.9 kcal mol^{-1}). The orbital stabilization energy, ΔE_{orb} in $Be(CO)_3$ and $Be(CO)_4$ are found to be −236.7 and −224.1 kcal mol^{-1}, respectively, which contributes significantly to the attractive component of the interaction energy (73.1% in $Be(CO)_3$ and 74.0% in $Be(CO)_4$).

The beryllium in the excited state with $1s^2 2s^0 2p_z^2$ electronic configuration has three vacant in-plane orbitals, which can form σ bonds with three CO ligands. Hence, the Be–C bonds in $Be(CO)_3$ can be considered formal 2c–2e bonds. However, the

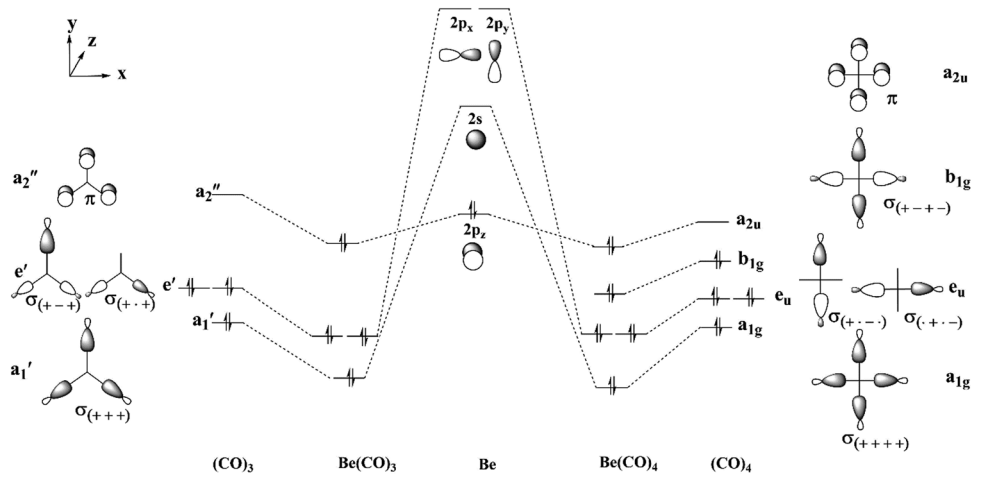

Scheme 2 Atomic orbitals of Be atom in the excited state ($1s^2 2s^0 2p_z^2$) interacting with ligands group orbitals of $(CO)_3$ and $(CO)_4$ fragments in $Be(CO)_3$ and $Be(CO)_4$.

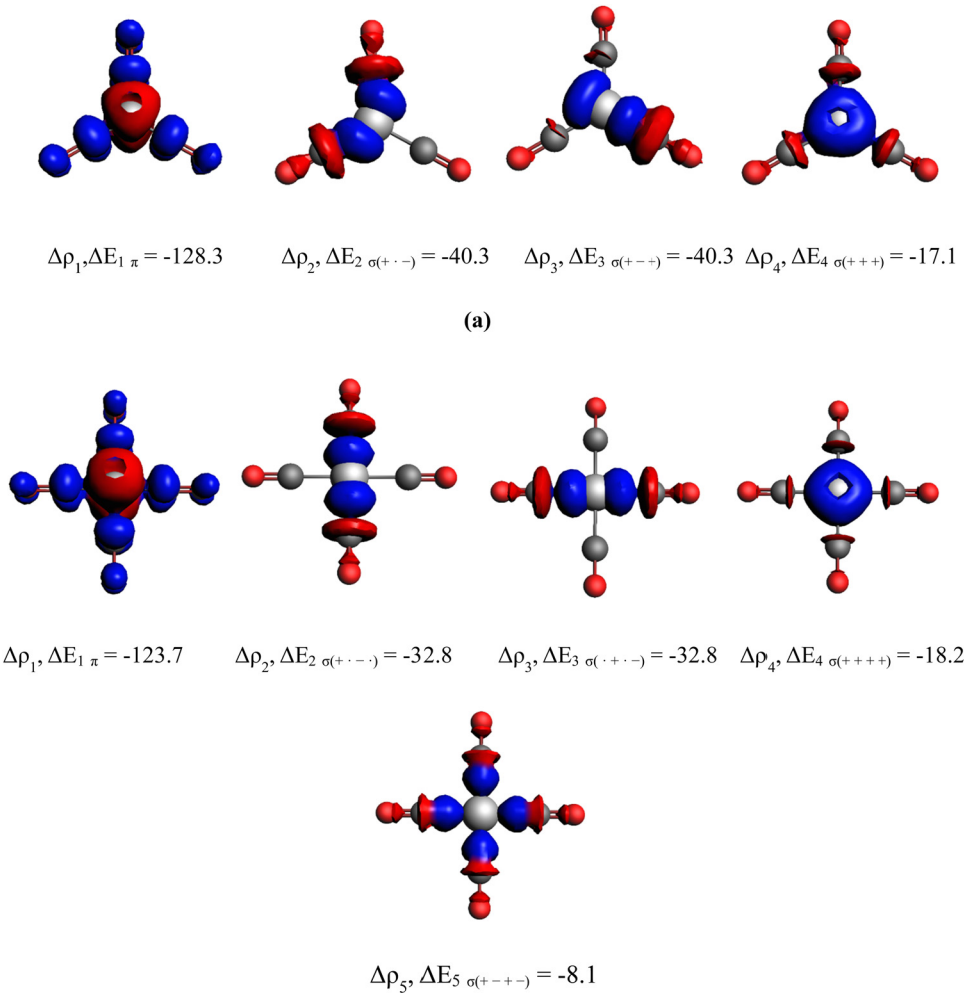

Fig. 3 (a) Plot of NOCV deformation densities ($\Delta\rho_1$ – $\Delta\rho_4$) and orbital interaction energies (kcal mol^{-1}) from each NOCV pair of $Be(CO)_3$. (b) A plot of NOCV deformation densities ($\Delta\rho_1$ – $\Delta\rho_5$) and orbital interaction energies (kcal mol^{-1}) from each NOCV pair of $Be(CO)_4$. The direction of the charge flow in the deformation density plot is from red → blue. The isosurface value for NOCV deformation densities is 0.003.

multicentre bonding concept needs to be invoked to explain four Be–C σ-bonds in $Be(CO)_4$. This is corroborated by the geometrical pattern where the Be–C bonds in $Be(CO)_3$ (1.655 Å) are shorter than those in $Be(CO)_4$ (1.811 Å).

To understand the variation in σ and π interaction among $Be(CO)_3$ and $Be(CO)_4$, we decomposed the ΔE_{orb} into the contribution from atomic orbitals of beryllium. Since $Be(CO)_3$ and $Be(CO)_4$ are perfectly trigonal planar (D_{3h}) and square planar (D_{4h}) molecules, the ligand group orbitals of $(CO)_3$ and $(CO)_4$ are similar to those shown in Scheme 1. The all (+) combination of the ligand group orbital (a'_1 for $Be(CO)_3$ and a_{1g} for $Be(CO)_4$) are right symmetry to interact with the 2s orbital of the Be atom. Note that the energy stabilization due to this interaction is only slightly higher for $Be(CO)_4$. The second σ(+ − +) and third set σ(+ · −) of the ligand group orbitals of $(CO)_3$ are right symmetry to interact with $2p_y$ and $2p_x$, respectively (Scheme 2).

The energy stabilization due to this interaction is more than two times that of the former interaction in $Be(CO)_3$ (Table 1). Hence, we wish to propose that 2p orbitals of beryllium atoms are better σ acceptors as compared to the 2s orbital. Similarly, the second σ(+ · − ·) and third σ(· + · −) set of ligand group orbitals of $(CO)_4$ also have the right symmetry to interact with $2p_y$ and $2p_x$ orbitals of the Be atom. The corresponding energy stabilization is lower than those in $Be(CO)_3$. Nevertheless, the energetics indicate that 2p orbitals are better σ acceptors as compared to 2s orbitals. The deformation densities corresponding to σ and π interactions in both the systems are shown in Fig. 3. $\Delta\rho_2$ – $\Delta\rho_4$ shows the accumulation of red region around ligand group orbitals along with an accumulation of blue region in the direction of 2s/2p orbitals of central Be atom. Thus, the flow of charge density from red → blue reaffirms σ donation from CO ligands to the Be centre.

The fourth combination of ligand group orbital of $(CO)_4$ does not have a right symmetrical orbital to interact with beryllium. The energy stabilization for this interaction arises from the polarization of ligand orbitals towards a more electropositive

beryllium centre. The total orbital stabilization energy due to σ-donation from the CO group in $Be(CO)_3$ is −97.7 kcal mol^{-1}, whereas the corresponding value for $Be(CO)_4$ is −91.9 kcal mol^{-1}. The π-back donation from central Be atom to CO ligands (ΔE_π = −128.3 kcal mol^{-1} and −123.7 kcal mol^{-1} in $Be(CO)_3$ and $Be(CO)_4$ respectively) considerably predominates over the σ donation for both $Be(CO)_3$ and $Be(CO)_4$. The deformation density $\Delta\rho_1$ in Fig. 3 represents a π-back donation from the $2p_z$ orbital of Be to the π-symmetric ligand group orbitals. Important NOCV pairs of orbitals Ψ_{-n}/Ψ_n associated with respective deformation densities are plotted in Fig. S1 and S2 of ESI.†

Conclusion

In summary, density functional calculations were carried out in the $Be(CO)_n$ (n = 1–4) complex. The present study predicts a stable beryllium carbonyl complex $Be(CO)_4$, which adopts perfect square planar geometry in its lowest energy singlet ground state. Detailed bonding analysis reveals that Be ← CO σ donation takes place at the vacant 2s, $2p_x$ and $2p_y$ orbitals of beryllium and Be → CO (π*) back donation takes place from the occupied $2p_z$ orbital of beryllium, thus exactly mimicking the DCD model for transition metal carbonyl complexes. The beryllium atom forms donor–acceptor bonds with four CO groups in its $1s^2 2s^0 2p_z^2$ electronic configuration. EDA analysis further elucidates the extent of σ and π interaction in $Be(CO)_{3-4}$. It is found that the stabilization energy associated with π-backdonation is considerably higher than that of σ-donation. The proposed $Be(CO)_4$ complex is stable and expected to be detected experimentally, which may be a low-temperature noble gas matrix. The present bonding situation may rationalize the formation of Be(0) compounds stabilized by σ donor/π acceptor ligands such as CO and cyclic(alkyl)(amino)carbene. We feel that the present bonding model may be considered as a p-orbital analog of the famous DCD model and will inspire the design of many alkaline earth metal organometallic complexes in their low oxidation states.[4–6]

Author contributions

S. K. P and A. K. G. performed all the calculations and A. K. G. wrote the draft. S. K. dedicates this article to his mother Mrs Kalpana Purkayastha. Shahnaz S. Rohman: methodology, data curation, writing and editing of EDA-NOCV results. Pattiyil Parameswaran: EDA data curation and analysis, writing – review, editing and interpretation of EDA results.

Conflicts of interest

The authors declare no conflict of interest.

Acknowledgements

Computational facility of Cotton University is acknowledged. P.P. thanks DST-SERB for research funding. S. S. R. is grateful to Science and Engineering Research Board (SERB) for the fellowship and funding under National Post-Doctoral Fellowship Scheme with reference no. PDF/2022/003034. P. P and S. S. R. also thank the Centre for Computational Modelling and Simulation (CCMS) at NITC.

References

1 M. J. S. Dewar, *Bull. Soc. Chim. Fr.*, 1951, **18**, C79.
2 *Modern Coordination Chemistry: The Legacy of Joseph Chatt*, ed. G. J. Leigh and N. Winterton, Royal Society, London, 2002.
3 G. Frenking and N. Fröhlich, *Chem. Rev.*, 2000, **100**, 717–774.
4 M. Arrowsmith, H. Braunschweig, M. A. Celik, T. Dellermann, R. D. Dewhurst, W. C. Ewing, K. Hammond, T. Kramer, I. Krummenacher, J. Mies and K. Radacki, *Nat. Chem.*, 2016, **8**, 890–894.
5 M. Chen, Q. Zhang, M. Zhou, D. M. Andrada and G. Frenking, *Angew. Chem., Int. Ed.*, 2015, **54**, 124.
6 S. A. Couchman, N. Holzmann, G. Frenking, D. J. Wilson and J. L. Dutton, *Dalton Trans.*, 2013, **42**, 11375–11384.
7 S. De and P. Parameswaran, *Dalton Trans.*, 2013, **42**, 4650–4656.
8 J. Tao, J. P. Perdew, V. N. Staroverov and G. E. Scuseria, *Phys. Rev. Lett.*, 2003, **91**, 146401.
9 Y. Zhao and D. G. Truhlar, *Theor. Chem. Acc.*, 2008, **120**, 215.
10 M. J. Frisch, G. W. Trucks, H. B. Schlegel, G. E. Scuseria, M. A. Robb, J. R. Cheeseman, G. Scalmani, V. Barone, G. A. Petersson, H. Nakatsuji, X. Li, M. Caricato, A. V. Marenich, J. Bloino, B. G. Janesko, R. Gomperts, B. Mennucci, H. P. Hratchian, J. V. Ortiz, A. F. Izmaylov, J. L. Sonnenberg, D. Williams-Young, F. Ding, F. Lipparini, F. Egidi, J. Goings, B. Peng, A. Petrone, T. Henderson, D. Ranasinghe, V. G. Zakrzewski, J. Gao, N. Rega, G. Zheng, W. Liang, M. Hada, M. Ehara, K. Toyota, R. Fukuda, J. Hasegawa, M. Ishida, T. Nakajima, Y. Honda, O. Kitao, H. Nakai, T. Vreven, K. Throssell, J. A. Montgomery, Jr., J. E. Peralta, F. Ogliaro, M. J. Bearpark, J. J. Heyd, E. N. Brothers, K. N. Kudin, V. N. Staroverov, T. A. Keith, R. Kobayashi, J. Normand, K. Raghavachari, A. P. Rendell, J. C. Burant, S. S. Iyengar, J. Tomasi, M. Cossi, J. M. Millam, M. Klene, C. Adamo, R. Cammi, J. W. Ochterski, R. L. Martin, K. Morokuma, O. Farkas, J. B. Foresman and D. J. Fox, *Gaussian 16, Revision B.01*, Gaussian, Inc., Wallingford CT, 2016.
11 F. Neese, *Wiley Interdiscip. Rev.: Comput. Mol. Sci.*, 2018, **8**, e1327.
12 F. Neese, F. Wennmohs, U. Becker and C. Riplinger, *J. Chem. Phys.*, 2020, **152**, 224108.
13 B. Silvi and A. Savin, *Nature*, 1994, **371**, 683–686.
14 A. D. Becke and K. E. A. Edgecombe, *J. Chem. Phys.*, 1990, **92**, 5397–5403.
15 T. Lu and F. Chen, *J. Comput. Chem.*, 2012, **33**, 580.
16 (*a*) K. Morokuma, *J. Chem. Phys.*, 1971, **55**, 1236–1244; (*b*) L. Zhao, M. Hermann, W. H. E. Schwarz and G. Frenking, *Nat. Rev. Chem.*, 2019, **3**, 48–63.

17 A. Michalak, M. Mitoraj and T. Ziegler, *J. Phys. Chem. A*, 2008, **112**, 1933–1939.
18 A. D. Becke, *Phys. Rev. A: At., Mol., Opt. Phys.*, 1988 **38**, 3098.
19 (*a*) *ADF2020.102, SCM, Theoretical Chemistry*, Vrije Universiteit, Amsterdam, **https://www.scm.com**; (*b*) G. te Velde, F. M. Bickelhaupt, E. J. Baerends, C. F. Guerra, S. J. A. van Gisbergen, J. G. Snijders and T. Ziegler, *J. Comput. Chem.*, 2001, **22**, 931–967.
20 L. Andrews, T. J. Tague, G. P. Kushto and R. D. Davy, *Inorg. Chem.*, 1995, **34**, 2952–2961.
21 K. K. Sunil, *J. Am. Chem. Soc.*, 1992, **114**, 3985.
22 X. Wu, L. Zhao, J. Jin, S. Pan, W. Li, X. Jin, G. Wang, M. Zhou and G. Frenking, *Science*, 2018, **361**, 912–916.